

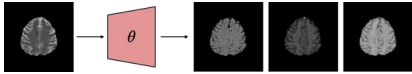
Generation of Multi-modal Brain Tumor MRIs with Disentangled Latent Diffusion Model



Yoonho Na, Kyuri Kim, Hwiyoung Kim, Sung-Joon Ye and Jimin Lee

Introduction

- Prior researches generating multi-modal MRIs rely on Image-to-Image translation and thus require **source image** to obtain fixed structural information.



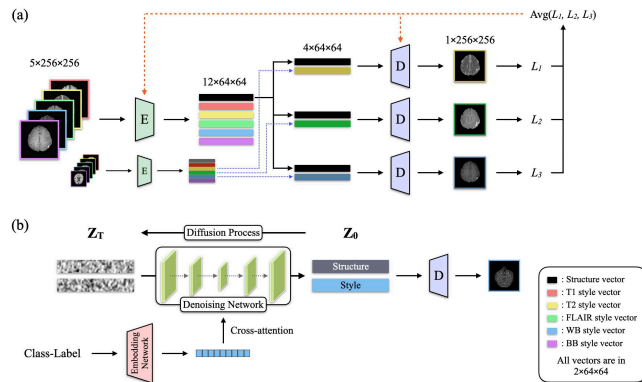
- Image-to-Image translation based approach has limitation that the structural diversity is restricted to the source image.
- We propose a novel approach for generating multi-modal brain tumor MRIs using feature disentanglement and diffusion models.
- Our proposed model, which we call disentangled latent diffusion model (DLDM), is capable of generating **modality-sharing** and **modality-specific** information separately, eliminating the need for source image.

Methods

Key Idea

- Extract modality-sharing information from the multi-modal MRIs.
→ Brain structures
- Decoding the latents with the fixed modality-sharing informations results in images with fixed brain structures.

Overview



DLDM is based on *Latent Diffusion Model* (Rombach et al., 2022).

Therefore our proposed model require two steps for training.

- Train autoencoder that maps pixel space to lower dimensional latent space
- Train diffusion model that operates in learned latent space of autoencoder

Step 1 : Disentangled Autoencoder

Training Strategy

- For N number of MRI modalities, set the dimension of latent vector dimension to have $N+1$ channels.
 - Each N channels to have N distinct style vectors z^{style} and the rest channel to have structure vector z^{struct} .
- Feed z^{struct} and randomly selected single z^{style} to the decoder.
- Randomly mix z^{style} with other data in mini-batch.
 - Strategy 2 and 3 ensures the encoder to separate multi-modal MRIs into modality-sharing and modality-specific information.
- Average the loss of selected modalities to ensure every modalities having similar reconstruction quality.

$$L_{Autoencoder} = L_{rec}(x, \mathcal{D}(\mathcal{E}(x))) + L_{reg}(x; \mathcal{E}, \mathcal{D})$$

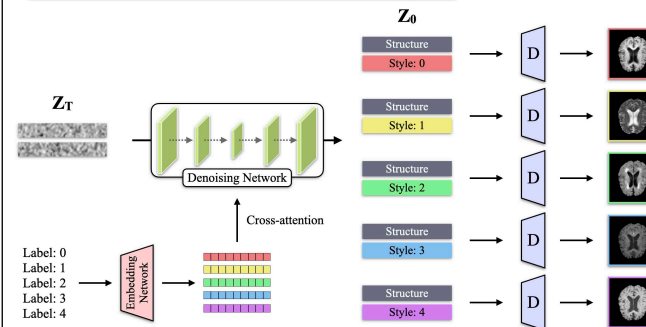
Step 2 : Disentangled Latent Diffusion Model

Training Strategy

- We use the pair of (z^{struct}, z^{style}) as a input of latent diffusion model.
- Class-label c , is applied as condition to selectively obtain z^{style} for every MRI modalities.
- When sampling multi-modal MRIs, we fixed z^{struct} to generate same structural data.

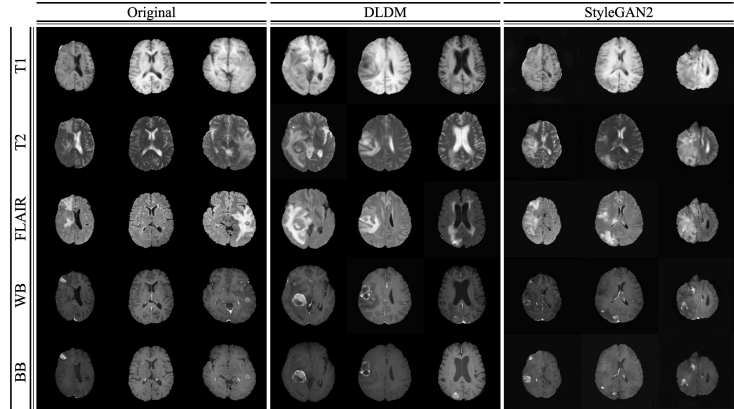
$$L_{DLDM} := \mathbb{E}_{\mathcal{E}(x), c, \epsilon \sim \mathcal{N}(0,1), t} \left[\left\| \epsilon - \epsilon_{\theta}(z_t^{struct}, z_t^{style}, \tau_{\theta}(c), t) \right\|_2^2 \right]$$

Generation Process of Multi-modal MRIs



Experimental Results

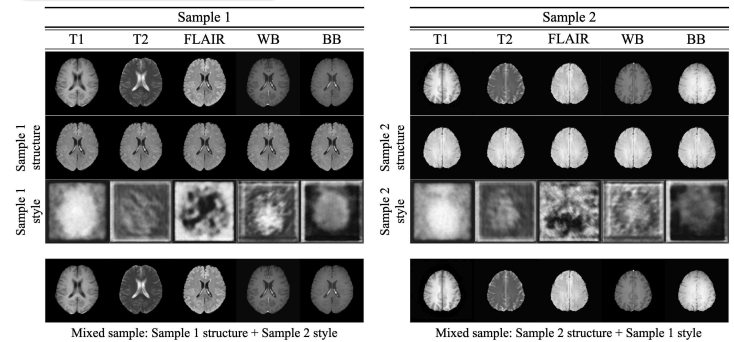
Qualitative Comparison



Quantitive Comparison

| DLDM | | | | | | | StyleGAN2 | | | | | | |
|----------|----------------|----------------|----------------|----------------|--------------|----------------|-----------|----------------|----------------|----------------|----------------|--------------|----------------|
| Modality | Precision↑ | Recall↑ | Density↑ | Coverage↑ | FID↓ | clean-FID↓ | Modality | Precision↑ | Recall↑ | Density↑ | Coverage↑ | FID↓ | clean-FID↓ |
| T1 | 0.95729 | 0.94063 | 0.96063 | 0.96563 | 18.52 | 0.00019 | T1 | 0.91042 | 0.72500 | 0.74125 | 0.84063 | 53.55 | 0.00284 |
| T2 | 0.90104 | 0.97083 | 0.81646 | 0.93438 | 13.86 | 0.00268 | T2 | 0.27708 | 0.50000 | 0.10792 | 0.25625 | 169.12 | 0.00385 |
| FLAIR | 0.87604 | 0.95417 | 0.77854 | 0.93646 | 25.49 | 0.00025 | FLAIR | 0.96250 | 0.46146 | 1.13708 | 0.87188 | 102.65 | 0.00208 |
| WB | 0.91146 | 0.95833 | 0.79896 | 0.92708 | 22.34 | 0.00018 | WB | 0.77500 | 0.75729 | 0.64937 | 0.85208 | 42.91 | 0.00260 |
| BB | 0.91458 | 0.97708 | 0.82458 | 0.90833 | 28.89 | 0.00022 | BB | 0.46354 | 0.96771 | 0.18625 | 0.38646 | 119.40 | 0.00328 |
| Average | 0.91208 | 0.96021 | 0.83583 | 0.93438 | 21.82 | 0.00070 | Average | 0.67771 | 0.68229 | 0.56437 | 0.64146 | 97.53 | 0.00293 |

Disentanglement Study



- Multi-modal MRIs are successfully disentangled into structure and styles.

Acknowledgments

This research was supported by a grant of the Korea Health Technology R&D Project through the Korea Health Industry Development Institute (KHIDI), funded by the Ministry of Health & Welfare, Republic of Korea (grant number: HI21C1161).